By

Amna Arif

00000276615/MSEE24

Supervisor

Dr. Abdul Wakeel

Department of Electrical (Telecom) Engineering,

Military National University of Sciences and Technology

(NUST),Islamabad, Pakistan

November 2021

LDPC code concatenation with Trellis shaping for PAPR reduction in OFDM systems

By

Amna Arif

A thesis submitted in conformity with the requirements for the degree of *Master of Science* in *Electrical (Telecom) Engineering*, Department of Electrical (Telecom) Engineering, Military College of Signals (MCS), National University of Sciences and Technology (NUST), Islamabad, Pakistan

Thesis acceptance certificate

Certified that final copy of MS/MPhil thesis written by MS/MR NS Amna Arif, Registration No. 00000276615 of Military College of Signals has been vetted by undersigned, found complete in all respect as per NUST Statutes/Regulations, is free of plagiarism, errors and mistakes and is accepted as partial, fulfillment for award of MS/MPhil degree. It is further certified that necessary amendments as pointed out by GEC members of the student have been also incorporated in the said thesis.

Signature:_____

Name of Supervisor: Asst Prof Abdul Wakeel, PhD

Date:_____

Signature (HoD): _____

Date: _____

Signature (Dean): _____

Date:_____

Declaration

I, *Amna Arif* declare that this thesis titled "LDPC code concatenation with Trellis shaping for PAPR reduction in OFDM systems" has not been submitted before for any degree application at NUST or any other educational institute. This synopsis is presented as a result of my own original research.

Amna Arif

00000276615/MSEE24

Copyright Notice

Dedication

I dedicate this thesis to my parents and my brother who are my constant pillars of strength in every walk of life. Its because of them that I'm able to achieve so much in life and more to come In shaa Allah.

I would also like to eminently dedicate this to *myself* for not giving up and showing up right till the end.

Abstract

Orthogonal Frequency Division Multiplexing (OFDM) systems are time and again incorporated in modern high-speed communication networks due to an increase in demand of reliable and error-free data transmission. OFDM is a propitious technique for efficient and reliable data transmission. Having said that,one major issue in OFDM systems is its signal's high dynamic range expressed as the peak to average power ratio (PAPR). In case the signal peaks are found higher than the linear operating range of the non-linear device they are passing through, these peaks are clipped off resulting both in-band distortion and out-of-band radiation. Clipping and Filtering, Tone Reservation (TR), Selected Mapping (SLM), Partial Transmit Sequences (PTS), Tone Injection (TI), Active Constellation Expansion (ACE) and Trellis Shaping (TS) are some of the procedures used for PAPR reduction, everyone with their own pros and cons. However, TS has been found efficient in terms of PAPR reduction without any increase in the mean power of the transmit signal for moderate computational complexity.

To further improve the system performance, herein, we propose TS using shaping codes of higher depths. Using shaping codes of higher depths improve the PAPR reduction as well the BER of the system. Moreover, we concatenate an optimized LDPC code with Trellis shaping. For the LDPC code, the variable node degree distribution is optimized based on the error probabilities of the individual bits inside a QAM constellation along with the error probabilities of the shaping code used. Simulation results show that the proposed technique has better PAPR reduction as well better BER as compared to the already existing systems using Trellis shaping with a shaping code of 4 states concatenated with an optimized

LDPC code.

Keywords: *OFDM, Trellis shaping, PAPR reduction, LDPC, constellations,shaping convolutional codes coded modulation, Normalized instantaneous power, varying trellis depths, LDPC code concatenation*

Acknowledgments

First of all, thanks to Almighty Allah who showered His countless blessings upon me and gave me the potential and aptness to understand and complete this research work.

I am truly indebted to my supervisor *Dr. Abdul Wakeel* for his constant encouragement throughout the duration of my research work.This work wouldn't have been possible without his unwavering support.

Contents

List of Figures

List of Tables

List of Abbreviations

Abbreviations

OFDM	Orthognal Frequency Division Multiplexing
PAPR	Peak to Average power ratio
BER	Bit Error rate
WiMAX	World-Wide inter-operability for Microwave access
LTE	Long Term Evolution
SNR	Signal to noise ratio
LDPC	Low Density Parity Check codes
VA	Viterbi algorithm
SISO	Single Input Single Output
MIMO	Multiple Input Multiple Output
CP	cyclic prefix
ISI	Inter symbol Interference
ICI	Inter channel Interference

Chapter 1

Introduction

Major reforms in the world are attributed to the advancements and progressions in electronic communication [1]. In the previous years, communication with someone was quite tiresome and was only possible physically. However, now connecting with someone or sending a piece of information is just a click away. Wireless communication is the conveyance of information without the use of wires [2]. Wireless communication techniques range from smoke signals and semaphores to satellite communication and beyond. Initially, when the radio fell out of fashion, the term wireless communication was coined and revived when the cellular telephony advancements began. Nowadays, wireless communication is majorly associated with Electromagnetic (EM) waves which groups it mainly into the scope of electrical communication [3].

Major classifications of wireless communication are that they are either analog or digital in nature. Commercial systems such as Amplitude Modulated (AM)/ Frequency Modulated (FM) radio, television and first-generation cellular systems designed earlier were purely analog [4]. In the present world, digital communication systems, where the source is digital, has taken over the analog communication systems.

Transmitter and receiver are the two main parts of a digital communication system. Transmitter sends a data stream which is received by a receiver. Most often, the data received is not what was sent initially by the transmitter. Amongst other

reasons, the signal is corrupted due to the presence of noise in the transmission medium. It is nearly impossible to receive a signal that is exact replica of the signal transmitted but modulation techniques are used to get a signal close to the originally transmitted signal. Traditionally, wireless communication was not much developed due to its limited use. Over the last few decades, market has observed a tremendous increase in the need of low cost and low power wireless technology. Furthermore, these equipment must also be in-line with the various wireless communication standards.

Every module including the Radio frequency (RF) and base-band necessarily require to incorporate wireless standards for global systems for mobile communications (GSM) [3, 4]. At present, the most sought-after cellular telecommunication system globally is GSM. According to a survey, a decade ago only 1 billion people used wireless communication as a data transfer mode. However, now this number has rose to more than 10 billion devices and is growing exponentially over time. This exponential increase in wireless data traffic over the years has opened ways for new and improved wireless data communication techniques. However, this will require a huge paradigm shift in the existing mechanization to meet the ever increasing demands of the required high carrier frequency bands, base station densities, and unequalled number of antennas to support the rise in the traffic magnitude.

For this specific framework, orthogonal frequency division multiplexing (OFDM) is considered as the premier physical layer technologies that can be incorporated in future wireless communication technologies. Reason being that OFDM provides unprecedented solutions to accomplish the goal of higher data rates in wireless communication [5]. OFDM is a physical layer transmission scheme of the long term evolution (LTE) and Worldwide Interoperability for Microwave Access (WiMAX) standards[6]. However, OFDM has very high peaks with respect to its average (PAPR), which is a practical limitation in its use [7]. The subcarriers number in OFDM increases with increase in its portability and data rates. As the signals of multiple sub-carriers adds up constructively, this causes in an increase in the peak powers of the signal. Almost all wireless communication modules are peak power

limited, techniques that mitigate high PAPR needs to be developed. This issue spur new research activities in the field of OFDM and wireless communication.

1.1 Motivation

OFDM is a widely used communication technology because of its numerous benefits in long distance communication and high gains. However, a significant pitfall of OFDM is the high PAPR. All electronic devices (for instance high power amplifier (HPA)) have different thresholds to operate in its linear region, which means that when an OFDM signal passes through such devices, distortion in the signals is observed because they are driven in the nonlinear operation range. Therefore,high PAPR issue needs to be addressed to make OFDM one of the most promising technologies for the upcoming communication systems. Therefore, the problem of high PAPR needs to be addressed and counter measures must be taken to restrain the unwanted peak excursions in OFDM systems. Thus, PAPR reduction has received significant attention over the past years. Many researches are working to develop efficient algorithms for PAPR reduction.

1.2 Problem statement

In this thesis, we consider Trellis shaping (TS) amongst all the available techniques for PAPR reduction because of its high efficiency and reduced complexity. Communication systems widely use OFDM technology but its high PAPR issue tends to be the main hurdle in its way to become state-of-the art technology for today's modern digital communication. Through out the literature, the authors have used shaping codes with a small constraint length (thus less number of states), i.e., usually using a 4-state shaping code. In his base paper on trellis shaping [40], Forney has shown that the shaping gain increases with the increase in the trellis depth. Moreover, it has also been found in the literature that the BER performance of the convolutional codes is also increased as the constraint length increases (more

memory units, i.e., higher states). Therefore, for trellis shaping, we consider different shaping codes of high constraint length (Trellis depth). This will result in performance improvement with regard to PAPR reduction. Moreover, we will also evaluate BER results of different shaping codes used. For further improvement of the system performance in term of BER, we will concatenate irregular LDPC code optimized for the different shaping code used. This improvement in PAPR reduction will make OFDM system the most promising digital communication technique for the next generation wireless networks.

1.3 Previous Contributions

The modulation of multiple data bits is carried out by multiple carrier frequencies. For this,the entire transmission band is sub divided into narrower sub-bands. Afterwards these sub-bands are assigned to each data symbol [8]. To keep away from the effects of frequency-selective fading, OFDM sub-divides the broad transmission band into narrower sub channels. According to researchers, for the fixed and mobile high speed wireless systems, OFDM is expected to out-perform other proposed wireless technologies. However, the snag that occurs in OFDM is its derived varying envelope with high peaks [9]. It has been found that the instantaneous peak power in time domain transmit signal is quite higher than the average power of the signal when subcarriers that are independently added-up constructively. Numerous strategies discussed previously for PAPR curtailment are mainly categorized as: Signal distortion, multiple signalling and probabilistic techniques. They aid in reducing the PAPR but inculcate in-band distortion and out-of-band radiation which causes an increase in the BER [9]. Application of these signal distortion techniques require great care as sometimes, peak cancellation at one point leads to a new peak formation at some other part of the signal. The multiple signaling and probabilistic techniques are based on generating various samples or frames of the original data and later choosing one with minimum PAPR for transmission. In theses techniques of PAPR reduction, differential encoding or the transmission of side-information about the phase-factor involved, and generation of multiple

copies of the same signal, therefore,its computational complexity is higher. Finally comes the coding techniques of PAPR reduction; Coding approach causes no distortion but the problem here is that it has issues in bandwidth efficiency as the information rate is reduced [10]. Some of the important coding techniques of PAPR reduction from literature are: Pre-coding, Linear block coding and Golay complimentary sequences. Theses coding schemes tend to provide desirous PAPR reduction when added to error-detecting codes. However, complexity increases many folds. Apart from complexity, the choice of most appropriate code and their storage in lookup tables is quite tedious in case of large number of sub-carriers.

1.4 Objectives

1 Evaluate the effects of using higher depth trellises for PAPR reduction.

2 Computation of error probability (P_b) of the individual bits of the shaping codes.

3 Optimization of degree distribution for variable nodes of an LDPC code depending on the bit error probability (P_b) for higher order $\mathcal{M}$-quadrature amplitude modulation ($\mathcal{M}$-QAM) constellations.

4 Design of irregular low density parity check (LDPC) codes sequenced with Trellis shaping for PAPR reduction.

1.5 Thesis road map

The thesis consists of 5 chapters and the details are as follows:

Chapter 1: This chapter gives a detailed introduction of the topic, brief overview of the issues contributions made before and the contributions of this report with relevance to national needs.

Chapter 2: This chapter contains the literature review. It explains the multi-carrier systems specifically Orthogonal Frequency Division Multiplication (OFDM) and its demand for modern day communication system. It also gives a detailed description of the existing work done on the PAPR reduction of OFDM systems. It also points out the drawbacks of each technique.

Chapter 3: This chapter briefly explains the existing PAPR reduction techniques already used. Moreover,Trellis shaping is discussed in detail as we incorporate TS technique for PAPR reduction in our work. Different branch metrics used for Trellis shaping are elaborated. A brief overview of metric selection criteria for PAPR reduction is also given.

Chapter 4: This chapter discusses the results of PAPR reduction for the higher depths trellises. The effects of LDPC code concatenation with trellis shaping is also evaluated along with the BER curves of OFDM signals.

Chapter 5: Here we discuss basics of BCJR algorithm and combined Trellises. The optimization of variable nodes and the degree distribution algorithm are also briefly discussed.

Chapter 6: Here we conclude the synopsis along with presenting the future work.

Chapter 2

Orthogonal Frequency Division Multiplexing

Communication around the globe for exchange of data, to express ideas and convey messages, has been the primary need of mankind since day one. The ancient history offer examples of physical communication including carrier pigeons, horse relays, and men who ran from place to place to carry information. The basis of today's wireless communication is the experiments carried out in the 17th and 18th centuries by the Chinese , Greeks, and Romans. It is also widely linked with their apprehension of electric and magnetic properties. The demonstration of radio's ability to enable communication with the sailing ships in 1897 by *Guglielmo Marconi* was the first major out-break in the communication world. The first wireless Telegraph and Signal company was founded and since then, with every passing day new and improved wireless communication methods and services are being introduced. The number of people using wireless communication technology is growing at an exponential rate. This rapid growth in the wireless technology users is due to advances in digital signal processing (DSP), digital switching techniques, RF circuit fabrication and large scale deployment of radio communication networks[11]. The basis of modern day wireless communication is rooted back to the older telegraphy systems, telephony, and radio technologies that were used back then. Wireless communication is also under the influence of newer communication capabilities that have affixed improved techniques for communication. The

government and regulatory bodies have assigned unique transmission bands to all the wireless transmission organizations, i.e., they use separate frequency bands for transmission. The expeditious increase in the number of users spur new research opportunities for the improvement and increased efficiency of communication systems.These trends will continue at an even greater pace during the upcoming times. This rapid growth in the number of users makes it necessary to re-look at all aspects of networking from basic to advanced network architecture and data processing [12, 13].

2.1 Orthogonal Frequency Division Multiplexing (OFDM)

The conduct of business and entertainment has already leveled up due to the deployment of 3G and 4G mobile communication systems world-wide alongside access to information. They have dragged up the users from slow and inconvenient equipment's to high speed and mobile communication technologies [16]. The right bridge between internet and telephony is already developed. The thrive for transforming the dream of higher data rates and seamless connectivity is being materialized by the researchers efforts [17]. Spectrum efficiency has always been the go-to for wireless technology. For this purpose, many new researches are carried out each day and improved technologies are introduced. Amongst other technologies, OFDM has emerged as a favourable solution to cope with the ever-increasing demands of subscribers and to full fill the requirements of next generation networks (NGN) [18].

OFDM is a specific form of multi carrier (MC) communication. OFDM achieves high data rates by splitting up the channel into multiple sub channels that transmits data in parallel [17, 19]. Information is carried by closely spaced orthogonal subcarriers. The objective here is to modulate each subcarrier with a different modulation technique (for instance QPSK, QAM) but at a low symbol rate. The symbol rate is kept low so that it stays similar to the conventional single car-

rier modulation technique. The symbol duration in OFDM is increased to combat the Inter symbol interference (ISI). OFDM is a physical layer transmission scheme used world-wide. OFDM have numerous advantages and applications in wireless communication networks, 4G/5G mobile communication, digital video and audio broadcasting (DVB/ DAB) [19]. Besides, OFDM have a number of commercial applications for instance Digital Subscriber Line (DSL), DVB-H, and MediaFLO, e.t.c.. It bears high spectral efficiency, adaptable resource allocation and robustness against Inter-Symbol Interference (ISI). OFDM is of major importance because of its ability to deal with the issues of multi-path propagation, high data-rates, and bandwidth efficiency.

2.1.1 Fundamentals of OFDM

Modulation is referred to as the mapping of information by manipulating the amplitude, frequency and or phase of a high frequency carrier. Multiplexing, on the other hand, is sending multiple signals on a single channel hence sharing the available bandwidth with other independent channels [23]. In OFDM, a number of subcarriers are multiplexed and afterwards these multiplexed signals are transmitted on a channel as one main signal. In other words, first the data signal is divided into multiple independent subchannels followed by modulation and then the signals are re-multiplexed to form an OFDM signal ready for transmission. The use of multiple subcarriers instead of one is advantageous in many aspects. Overall system performance does not suffer due to the fault in one subcarrier

Discrete Fourier transform (DFT) is used to split entire available bandwidth into N subchannels for multi carrier transmission. In this way, multiple low bit rate streams are formed from a high data rate stream. These low data streams are then transmitted over different sub channels. OFDM signal carrying multiple modulated symbols are formed as a linear combination of complex exponential signals of finite time duration [24].

Let a complex symbol for transmission at the nth OFDM subcarrier be $(x_n, k)_{N-1}^{k=0}$

with $E|x_n, k| = \sigma_s^2$, mathematical representation of the OFDM signal is:

$$x_n(t) = \sum_{k=0}^{N-1} x_n, k^{e^{j2pik\Delta ft}}, \qquad 0 \leq t \leq T_s \tag{2.1.1}$$

where T_s shows the symbol duration, Δf for the sub-channel space and N for total number of subchannels, respectively.

Towards the receiving end, in case there is no distortion, the transmitted signal can be detected as

$$x_{n,k} = \frac{1}{T_s} \int_0^{T_s} x_n(t) e^{-j2pik\Delta ft} dt \tag{2.1.2}$$

For detection at the receiver, orthogonality condition must be satisfied. It states that length of symbol duration must be of enough length so that the subcarriers are orthogonal to each other for different values of K. Mathematically,

$$T_s \Delta f = 1$$

must be satisfied for orthogonality.

2.2 Discrete time OFDM - System model

OFDM system's block diagram is presented in the Fig. 2.1. Input data is initially mapped into an $\mathbb{M}$-ary Quadrature Amplitude Modulation (MQAM) symbol, i.e.,

$$X = [X_n], \qquad n = 1, 2, 3...., N \tag{2.2.1}$$

which is a transformation of the data into complex numbers, i.e.,

$$X_n = X_I(n) + jX_Q(n) \ , \tag{2.2.2}$$

where X_n is the nth $\mathbb{M}$-ary QAM constellation point. An additional feature of OFDM is that the same QAM constellation isn't necessary for all $[X_n]$ therefore, different modulation schemes can be used simultaneously. Bit loading and power loading are some of the modulation schemes used for various modulation schemes.

Later, through serial to parallel conversion, OFDM signal is generated. This converts the serial data into a parallel stream, i.e., $[X_n]^T$, where T represents the

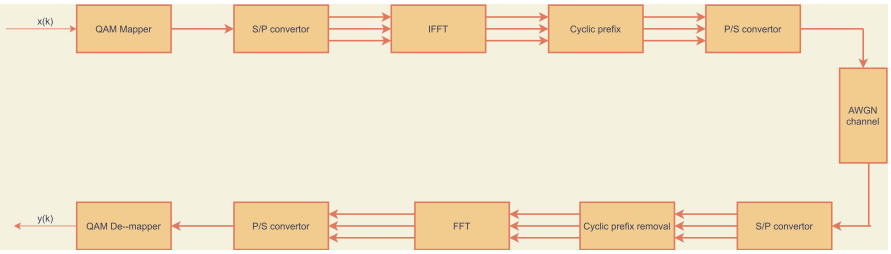

Figure 2.1: Main components of OFDM system

transpose. N-point IDFT (IFFT) modulator converts this data stream into time domain, such that:

$$[x_k] = IDFT[X_n] = \frac{1}{\sqrt{N}} \sum_{n=1}^{N} X_n e^{j} \frac{2\pi nk}{N}, \quad k = 1, 2, ...N \tag{2.2.3}$$

where x_k is for the kth sample while N shows the OFDM block length.An IDFT modulator converts the symbols into time-domain which are then re-converted to serial data by a parallel-to-serial (P/S) converter. Cyclic prefix (CP) is appended before transmission. First of all, cyclic prefix is removed at the receiver,the signal y_k is converted from serial to parallel data stream. DFT of the symbol is obtained. Lastly, the received symbols are demodulated as [25],

$$[Y_n] = DFT[y_k] = \frac{1}{\sqrt{N}} \sum_{k=1}^{N} [y_k] \ e^{-j} \frac{2\pi nk}{N}, \quad n = 1, 2, ..., N, \tag{2.2.4}$$

The received symbols DFT vector is shown by $[Y_n] = \mathbf{Y} = [Y_1, Y_2....., Y_N]$.
For the demodulation of the detected symbol at the receiver, the orthogonality condition must be fulfilled, i.e., $T_s \ \delta f = 1$. The transmitted symbol $x_{n,k}$ is received as:

$$x_{n,k} = \frac{1}{T_s} \int_0^{T_s} x_n(t) e^{-j2pik\Delta ft} dt \tag{2.2.5}$$

2.3 Peak-to-average-power ratio (PAPR)

OFDM is an extensively used transmission technique for remote communication because of its maximum bandwidth utilization and reduced ISI. But, a major drawback of OFDM is the high ratio of its peak power to the average power (PAPR), defined as, the ratio of the maximum peak power divided by the average

power of the time domain OFDM symbol. Its dynamic range being high is a major contributor to increased PAPR [32]. The sub-carriers of are out-of-phase and at each instant, they have varying phase values but at some point, they add up hence achieving maximum peaks simultaneously giving rise to 'high peaks'. Upon adding K signals of the same power, the peak power will be *K-times* that of the original signal power. This very high PAPR of OFDM system is sensitive to non-linearity of various high power amplifiers. The peak power of M-QAM modulated symbols is expressed as:

$$P_{QAM} = \frac{\alpha^2}{2}(\sqrt{M} - 1)^2 \tag{2.3.1}$$

where, α shows the Euclidean distance (minimum) while $\mathbb{M}$ is the size of constellation used. The average power of M-QAM modulated symbol is expressed as:

$$P_{QAM} = \frac{\alpha^2}{6}(M - 1) \tag{2.3.2}$$

Mathematically, the PAPR of an OFDM signal is expressed as:

$$PAPR(x) = \frac{Peak\ \ power}{Average\ \ power} = \frac{\max |x_k|^2,}{E|x_k|^2} \tag{2.3.3}$$

2.3.1 PAPR and CREST factor

In literature, sometimes PAPR is assumed to be similar to the crest factor but they are different and cannot be used interchangeably. Crest factor is a wave form parameter and is expressed as 'ratio of the peak values to the root mean square (r.m.s) value of the waveform'. This is usually used for voltages and alternating current wave forms. Crest factor is an indication of the extent of how high the peaks of a waveform are. Mathematically, it is expressed as: peak value over the root mean square (RMS) value of a waveform:

$$C_f(s(t)) = \frac{max\ |s(t)|}{max\ |s(t)^2|} \tag{2.3.4}$$

However, crest factor squared is the PAR.

$$PAR = C_f^2 \quad or \quad C_f = \sqrt{PAR} \tag{2.3.5}$$

PAR and Crest factor are equal when measured in dB.

2.4 CDF and CCDF analysis

Complementary Cumulative Distribution Function (CCDF) is used to measure the time duration a signal spends above the average power limit. The PAPR reduction in OFDM signals is analyzed from CCDF. It basically depicts the PAPR of an OFDM frame in comparison to a certain pre-defined threshold τ. Mathematically,

$$CCDF(PAPR) = P_r > \tau \tag{2.4.1}$$

For understanding the statistical analysis, let $X = [x_n]$ is input of $\mathbb{M}_a ry$ QAM symbols that are i.i.d distributed with variance is $\sigma_k^2 = [x_k x_k^*]$ and zero mean. Suppose $\curvearrowleft = IFFT[X]$

$$[pdf(x_k] = 2x_k e^{-|x_k|^2} \tag{2.4.2}$$

The CDF can then be formulated as:

$$CDF(\tau) = (CDF_{\tau k}(\tau))^N = (1 - e^{-\tau})^N \tag{2.4.3}$$

Chapter 3

PAPR reduction techniques

PAPR is a well known problem of multicarrier systems and has been worked out by many researchers for long. A complete review of different PAPR reduction techniques is well presented in [32]. Herein, we will provide a brief discussion to some of the well known approaches used for PAPR reduction in SISO-OFDM systems. Most of these techniques has recently been extended for PAPR reduction in MIMO-OFDM systems. We first start with the consequences of high PAPR followed by different algorithms been proposed for its reduction.

3.1 Consequences of high PAPR

OFDM essentially transmits information reliably at a higher rate as compared to the single carrier system. One major draw back of OFDM system is the high PAPR, the time domain transmit signal has high dynamic range, i.e., the the time domain transmit signal has sporadic peaks much higher than the average power of the signal. As most of the electronic circuits (e.g., A/D converters, HPA) are peak power limited, thus passing such a signal through these non-linear devices will result in signal clipping. Clipping of the signal results in signal distortion thus abase the system performance in terms of BER. Therefore, measures needs to be taken to mitigate high PAPR. The counter measure is either to operate the non-linear devices with high power back-offs. However, operating HPA with high

power backs is inefficient in terms of power efficiency. Alternative measures will be to limit these peak excursion before passing them through the non-linear devices. To limit the occurrence of high peaks, different algorithms have been proposed by different authors. Some of these approaches are discussed in the subsequent sections.

3.2 Signal Distortion approach

The crux of these technique is to reduce the PAPR of OFDM signals by distortion prior to sending the signal through the power amplifier (PA).

3.2.1 Clipping and filtering

It is one of the simplest and frequently used PAPR reduction technique for SISO-OFDM systems. In clipping, a threshold value is set initially. If the amplitude of any time domain sample is higher than the predefined threshold, it is clipped. The threshold value is in accordance with the High-power amplifier (HPA) limit.The threshold is determined by the D/A converter or High-power-amplifier (HPA). Clipping is a non-linear process resulting in in-band distortion and out-of-band radiation. If the signal is filtered after clipping, this will greatly reduce the spectral spreading. The in-band radiation, however, can lead to severe degradation of BER performance which cannot be mitigated through filtering [33]. Amstrong proposed 'Frequency domain filtering of the clipped signal', which comprises of two DFT(FFT) operations. The out-of-band radiation components are nullified by forward DFT that takes the signal back to Frequency domain (FD). The second IDFT again transform the signal to time domain (TD) for which input is the already clipped signal. The clipped signal is given as :

$$x^c = \begin{cases} x, & |x| \leq A_o \\ A_0 e^{j\ arg(x)}, & |x| \geq A_0 \end{cases} \tag{3.2.1}$$

where A_0 is the predefined threshold.

This approach shows prominent results for the out-of-band radiation components. However, this causes a problem of re-emergence of high peaks, thus, clipping and filtering have to be used iteratively to bring the peak values in the HPA linear range. The recursive clipping and filtering increases the computational complexity of the system. Clipping and filtering when used repeatedly, limits the distortion at each tone. It achieves fast convergence along with low PAPR and low BER [35]. When PAPR is below a certain threshold signal distortion is minimized. Here, desired PAPR is achieved after one or two iterations which is quite less as compared to 10 to 16 iterations of the conventional clipping method.

3.2.2 Peak windowing

An alternative approach for hard clipping is peak windowing. In the clipping approach, peaks exceeding the clipping limit (CL) are clipped off completely. In this method, a time domain windowing function is multiplied with signals that have large peaks. Hamming, Hanning, Gaussian shaped window, Cosine and Kaiser windows are the most commonly used windowing functions due to their spectral properties [36]. A specific window function is aligned with the signal samples in a way that its depths are aligned to the signal peaks and its low amplitude points are multiplied with the signal samples at the peaks for PAPR reduction. This gives a much smoother peak attenuation than clipping without much increase in the BER, hence, resulting in reduced distortion. Harish kumar Pal and Anand Kumar Singh in [36] introduced an advanced peak windowing (APW) technique which overcome the short comings of the traditional methods. In signals where peaks emerge within half of the window size, the traditional mechanism does not perform well. By increasing the window length, out-of-band radiation was reduced hence keeping BER in limit. The APW technique focuses on detecting high peak values and suppressing them whether they appear as single or consecutive peaks. This attenuates the peaks that occur within half of the window length.

3.2.3 Companding

Companding technique is usually used for speech signals but can be applied for OFDM signals for PAPR reduction as the peaks occur infrequently. Companding have reduced complexity as compared to the other techniques and its complexity does not vary with the change in number of subcarriers. The four major classifications of companding are: LST, LAST, NLST and NLAST. Other companding transforms that lie in these classes are thoroughly discussed in literature [37]. Another PAPR reduction technique is μ-law companding. In μ-law companding, high peaks are preserved low amplitude signals are enhanced. Here the peak power is kept unaltered while increasing the average power which leads to PAPR reduction. The companded signals after distortion is represented by:

$$x_c[n] = A\frac{\log(1+\mu(\frac{|x[n]|}{A})}{\log(1+\mu)}sgn(x[n])\ , \tag{3.2.2}$$

where μ is the companding parameter and A is the normalization constant. The retrieved signal is expanded before demodulation using the equation:

$$x_e[n] = A\frac{\exp[\frac{x[n]}{A\ \ sgn(x[n])}\ \ log(1+\mu)]-1}{\mu\ sgn(x[n])} \tag{3.2.3}$$

3.2.4 Peak cancellation

In this technique, after the IFFT block a peak cancellation waveform is generated for PAPR reduction. The scaling, shifting and subtraction of this waveform from the OFDM signal at points where the signal comprises of high peaks reduces the PAPR [38]. This band-limited waveform is only for peak cancellation and is not used for data transmission. This peak cancellation waveform is used anytime a high peak signal appears in the OFDM signal.The system model of peak cancellation in OFDM transmitter is shown in Fig **??**. It is important to be careful while performing peak cancellation so that no new peaks are generated.

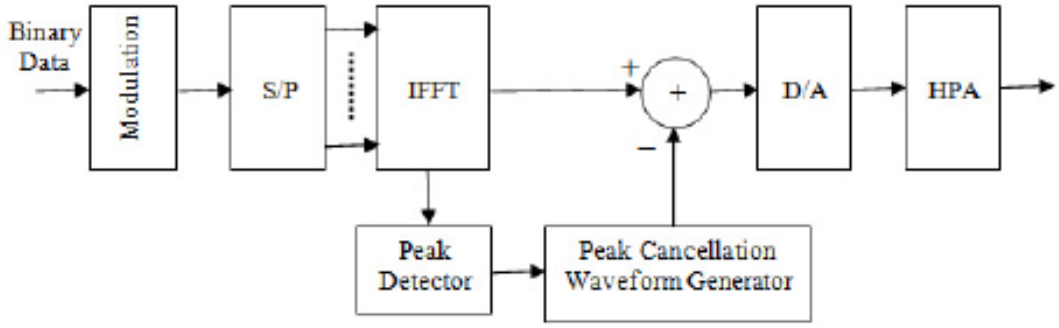

Figure 3.1: System model of peak cancellation.

3.3 Signal scrambling techniques

Signal scrambling techniques work in two ways. In the first method, the OFDM signal's permutations are created while in the second method, the OFDM signal is manipulated in certain ways. The modifications are made to reduce the PAPR of the OFDM signals. Some of these techniques are discussed here.

3.3.1 Selected mapping technique (SLM)

Bauml, Fischer, and Huber in 1996 proposed Selected Mapping (SLM) [57]. The basic working principle of SLM is to generate independent frames based on the original data. U statistically independent frames are generated from the original signal $X_{(m)}$, $0 \leq m \leq U-1$. The original data vector multiplied with U phasor vectors spawn these independent frames. The phase sequence representation is as follows:

$$\rho_k = [e^{j\sigma k,1} e^{j\sigma k,2}, ..., e^{j\sigma k,N}], \quad 0 \leq k \leq n-1, \tag{3.3.1}$$

where σ takes values from 0 to 2π excluding 2π.

The information that the independent frames carry is the same as that of the original data block. For generating a set of OFDM symbols, U different phase sequences P_m are element-by-element multiplied with the original OFDM frames $X = [X_1, X_2....X_N]$, each of length N before IDFT is performed. To choose the

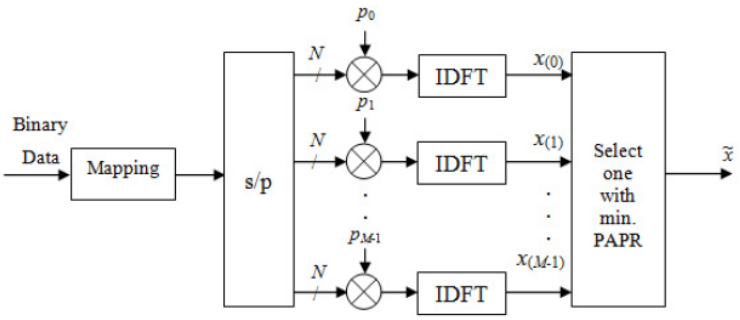

Figure 3.2: Selective mapping (SLM) Block diagram

frame with the least PAPR, the U-frames are converted to time domain and the frame that has the least PAPR is chosen for transmission [39].The transmitted OFDM frame is represented as:

$$x[n] = arg \ \ min \left[PAPR(x_{(m)})\right] \tag{3.3.2}$$

The simplest SLM block diagram is ac shown in Fig. 3.2

In case the QAM symbols are used as input to the OFDM systems, QAM symbols are rotated in the same constellation. The phase vectors are then set to $[\pm i, \pm j]$ for simplicity. The number of generated phase sequences U and their orientation determines the degree of PAPR reduction. The basic limitations of SLM are data rate loss and complexity at the transmitter. The system model of SLM is quite simple but complexity increases as the number of translated frames U increases.

3.3.2 Partial transmit sequence (PTS)

Muller and Huber in [58] proposed Partial Transmit Sequence (PTS). It works on the same principle as that of SLM. For PTS, an input data of N symbols is divided into D disjoint sub blocks. All the sub-carriers are weighted by a phase factor for that particular sub block. The selection of phase factor has a direct influence on the minimization of the PAPR of the combined signals belonging to any sub block. Each block is of the size N/D and is assigned a set of tones whereas all other tones are set to zero. Figure 3.3 shows the PTS block diagram. From the figure, we can see that the input data block is mapped before serial-to-parallel

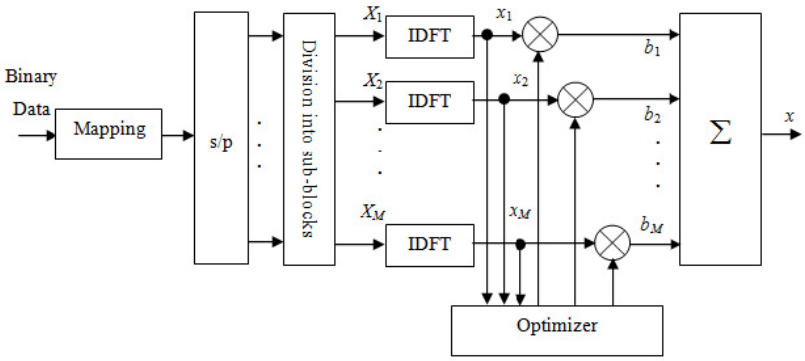

Figure 3.3: Partial transmit sequence (PTS) schematic

conversion. This entire data is then divided into sub blocks and IDFT of these blocks is performed. After optimization of all the sub blocks, the disjoint signals are combined before transmission.

The main difference in SLM and PTS is that in SLM, individual tones were rotated inside the frame while in PTS, each sub block has a defined rotation factor. PAPR of the combined signal is influenced by the phase factor chosen for rotation therefore it must be chosen carefully. Lastly, the sub block with the least PAPR are selected for transmission. PTS has improved performance over SLM but its computational complexity is comparatively higher. Apart from this PTS incorporates differential coding or has to send side-information about the phase-factor.

3.3.3 Interleaved OFDM

Interleaved OFDM basically is a concept which shows that if long correlations are broken, the PAPR will be reduced because long correlated signals have higher PAPR. Adaptive interleaving sets up an initial terminating threshold. The value of PAPR substantially decreases rather than seeking each interleaved sequence. The gain obtained using interleaved OFDM algorithm is not so prominent though the technique is less complex computationally.

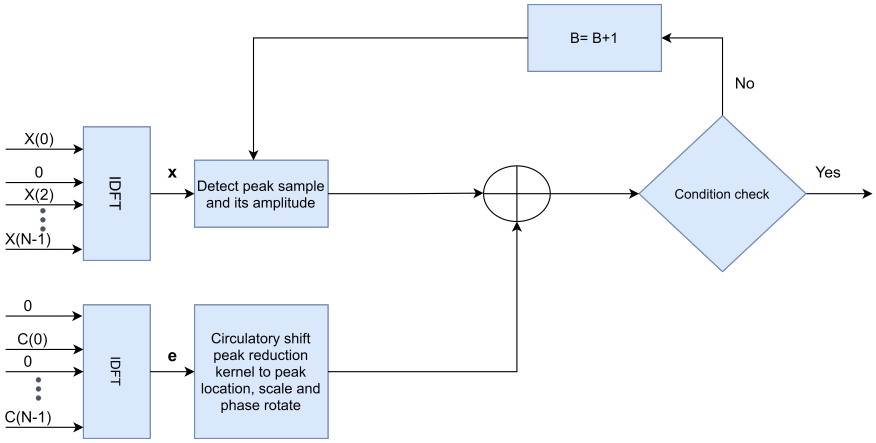

Figure 3.4: Tone reservation

3.3.4 Tone reservation

The TR algorithm was initially proposed by Tellado in [31,60]. The core idea was to have a set of tones dedicated entirely to PAPR reduction. Two different sets are made of the existing tones in an OFDM frame. One set of tones is then used for to transmit data. On the other hand,the second set is reserved for PAPR reduction. A function similar to Dirac is then generated on the reserved tones which are then added iteratively to the time domain transmission signal to reduce the PAPR. The Tone Reservation (TR) algorithm has the following main steps:

(1) The information vector $\mathbf{X}$ is initialized and the reserved tones are set to 0.

(2) $\mathbf{X}$ is transformed into time domain by taking its IFFT.

(3) The position $\lceil$ of the peak is identified.

(4) If $|x_d|$ is less than the pre-defined threshold, the process is terminated.Otherwise,

(5) The signal is modified before transmission according to:

$$x^{(i+1)} = x^i - \alpha(x_d^i - e^{j \arg x_d{}^{(i)}}.\tau)(r(N-m)moduloN) \tag{3.3.3}$$

i:= i+1 go back to step (3).

3.3.5 Tone Injection

It is an additive PAPR reduction approach. The main objective behind using additive approach is that it reduces the PAPR of multi-carrier signals without data rate loss. In tone injection method, before IDFT processing, the size of constellation is increased thereby allowing the mapping of original constellation from the complex plane to several other points of the expanded constellation [126, 129]. This freedom of choice in constellation mapping facilitates in PAPR reduction.This process is called tone injection because the replacement of an original constellation point by an extended constellation point is equivalent to the injection of a new OFDM tone.The new tone obviously having its own phase and frequency.

3.4 Trellis shaping (TS)

Initially, Trellis shaping (TS) was proposed for reduction of the average power by G.D Forney in [40]. However, it was later on extended for PAPR by Werner et. al. in [41]. In [41], the authors proposed two metrics, one in time domain and another in frequecy domain, as a branch metric for the trellis of the shaping code used. It was found that the time domain metric performs better than the frequency domain metric with added computational complexity as multiple DFT/IDFT pairs were used. TS is known to be the most flexible and appropriate PAPR reduction technique which can also be used to reduce the average power by controlling the transitions of the signals and exploiting the trellis codes structure. No side information transmission is required in trellis shaping and it is easily applicable in almost all systems. Unlike other PAPR reduction techniques, trellis shaping does not introduce any nonlinear distortion. For the application of TS for PAPR reduction, a technique with minimum complexity was developed that used auto-correlation of the side lobes of transmit signals in frequency domain by Ochiai in [45]. Trellis shaping requires constellation shaping like coded modulation but does not provide any error correction which shows that it relatively has a lower noise margin. Since our work is based on TS, a detailed explanation of TS will be

provided in the subsequent chapter.

Chapter 4

PAPR reduction using Trellis Shaping with different Trellis depths

Initially, G.D Forney, in [40], proposed TS for redusing mean power of the transmit symbols. The idea was later on extended for PAPR reduction by Werner et.al. in [41], where the authors proposed time domain and frequency domain solutions, however, the proposed solution was a bit complex. Ochiai proposed a frequency domain metric considering minimization of the auto-correlation of the side lobes, which is computationally less complex to the metrics proposed in [41]. Moreover, the authors in [41, 45] have used shaping codes with a small constraint length, i.e., usually using a 4-state shaping code. In his base paper on trellis shaping [40], Forney have shown that the shaping gain increases as the number of states of the shaping code increases. Therefore, for trellis shaping, we consider different shaping codes of high constraint length (Trellis depth/ higher number states). This will result in performance improvement in terms of PAPR reduction of an OFDM system.

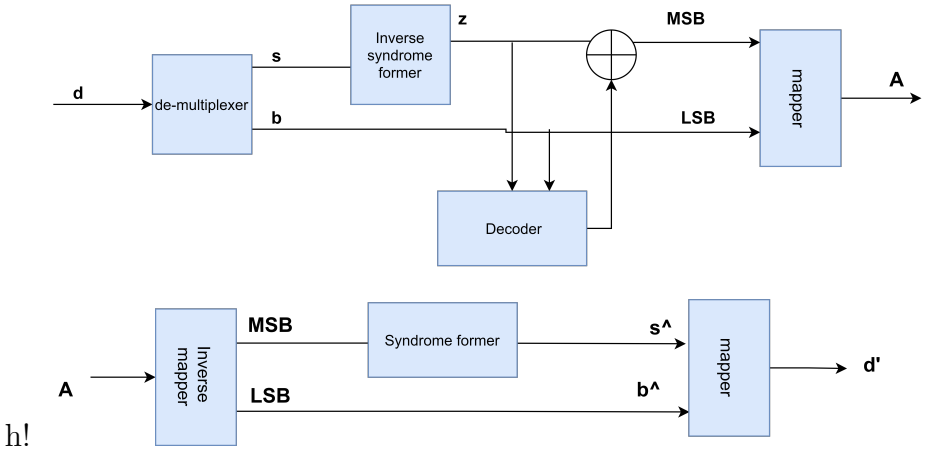

Figure 4.1: Block diagram of Trellis shaping

4.1 System Model

A basic structure of Trellis shaping technique is as shown in 4.1.

Let's, $\mathbf{G}$ be the generator matrix, $\mathbf{H^T}$ be the syndrome former and $(\mathbf{H^{-1}})^\mathbf{T}$ as left inverse of the syndrome former of a shaping convolutional code $\mathbf{C}_S$. $\mathbf{C}_S$ is the shaping code which is usually a convolutional code with rate $1/n_s = 1/2$, where n_s is the total output count of the convolutional code. Let's $\mathbf{G}$ be the $1 \times n_s$ generator matrix of the shaping code and $\mathbf{H}^T$ denotes the $n_s \times (n_s - 1)$ parity check matrix whereas, $(\mathbf{H}^{-1})^T$ represents the $(n_s - 1) \times n_s$, i.e., the left inverse matrix of the code.Here, a 1/2 rate convolutional code is employed as a shaping code, with $n_s = 2$.

Now lets suppose $\mathbf{d}$ represents the data-word to be transmitted by an OFDM system. The data sequence at the transmitter is demultiplexed into two disjoint sets, i.e., $\mathbf{s}$ and $\mathbf{b}$. Set of bits $\mathbf{s}$ is then used to form the MSBs for mapping $\mathcal{M}$-QAM while $\mathbf{b}$ chooses the LSBs [42]. Before the MSBs are chosen, using the $(\mathbf{H}^{-1})^T$ the $\mathbf{s}$-bit sequence is encoded to get $\mathbf{z}$, i.e.,

$$\mathbf{z} = \mathbf{s}(\mathbf{H}^{-1})^T \tag{4.1.1}$$

This output sequence $\mathbf{z}$ generated is modulo-2 added to $\mathbf{y}$, a valid codeword in C_s, i.e., $\mathbf{z} \oplus \mathbf{y}$. AT the receiver side, if correct data is received, then, the syndrome

former retrieves the dataword $\mathbf{s}$ as follows:

$$(\mathbf{z} \oplus \mathbf{y})\mathbf{H}^T = \mathbf{s}\,(\mathbf{H}^{-}1)^T\mathbf{H}^T \oplus \mathbf{y}\,\mathbf{H}^T = \mathbf{s} \oplus \mathbf{0} = \mathbf{s} \tag{4.1.2}$$

The constellation of the kth subscriber is then given by:

$$A_K = \mathcal{M}(\mathbf{z}_k + \mathbf{y}_k, \mathbf{b}_k) \tag{4.1.3}$$

where $\mathbf{z}_k$ corresponds shaping symbol and y_k corresponds to the output of the shaping decoder.

4.1.1 Sign bit shaping

Sign bit shaping begins with a square constellation such as 16×16 constellation. Each coordinate of this constellation takes up values from the 16-point PAM constellation $\pm\frac{1}{2}, \pm\frac{3}{2}, ... \pm\frac{15}{2}$ if this constellation is scaled in a manner that the minimum distance d_{min} is 1. Each coordinate's value is represented by "zabc.1" in two's complement notation. Here z is the most significant sign bit. As for the remaining bits abc, they are marked as the least significant bits. Each 2-bit output of the shaping code are used as MSBs, which chooses one out of the four quadrants of the $\mathcal{M}$-QAM constellation [45]. Moreover, over here, we consider Gray mapping for the $\mathcal{M}$-QAM constellation known as Type-1 in [45].

4.1.2 Constellation mapping for sign bit shaping

Rate 1/2 convolutional codes are considered for sign bit shaping. $(H^{-1})^T$ encodes the data sequence $\mathbf{s}$ to yield a binary sequence $\mathbf{z}_k$. A well founded code word $\mathbf{y}$ is added to $\mathbf{z}_k$. As $\mathbf{z}_k$ and $\mathbf{y}_k$ are both 2-bit symbols, the MSB chooses a quadrant from the $\mathcal{M}$-QAM constellation. As far as the LSBs are concerned, Type-1 mapping is considered. In Type-1 mapping, the 4 points in the equivalent class form a symmetry with respect to both the axes. As MSB chooses same energy points, this mapping lacks average power reduction capability. This makes it best suitable for PAPR reduction and its evident from the results that Type-1 mapping offers significant PAPR reduction as shown in [33].

The other LSB mapping technique known as Type-2 mapping is designed such that it have identical quadrants. Here, the shaping decoder can choose different energy points for any LSB hence providing average power reduction capability. To ensure the Bit-error-rate (BER) minimization of an uncoded system, both mappings ensure Gray mapping. For our simulation we consider Type-1 mapping for PAPR reduction only.

4.2 Metric selection for PAPR reduction

The strategy of metric calculation for the shaping decoder utilized for PAPR reduction in trellis shaping is crucial. Different metrics have been proposed for Viterbi algorithm in literature. These metrics are both in time and DFT domain. A valid branch metric should be positive and additive [44]. In [41], the transmit signal's peak power was chosen as the branch metric (time domain) for searching a valid code sequence in the shaping code C_s. However, this metric somehow does not accomplish the requirements of a branch metric because peak power is not additive. This metric applies the PAR criterion directly to the code sequence. The T.D peak power is calculated at each path and updated accordingly:

$$x_{k_v} = x_{k_{v-1}} + \sum_{(n=v-1)l+1}^{vl} X_n e^{j(\frac{2\pi}{N})^{KN}} \tag{4.2.1}$$

This branch metric have exceptional results but its computational complexity is quite high. In DFT domain, an alternative branch metric was proposed in [41], that was dependent on the phase of the symbols and block transition matrix's tabulation. However, this method was applicable only to small block sizes. Another branch metric proposed for papr reduction for viterbi algorithm takes into account the aperiodic auto correlation of the side lobes of OFDM signals[45] which is mathematically expressed as:

$$\lambda(y_k) = \sum_{m=1}^{kn_s-1} |\rho_m| \tag{4.2.2}$$

This is the widely used branch metric for search of a valid code sequence C_s.
Besides, another metric was proposed by Ochiai in [45] i.e. minimizing the sums

of squares of auto-correlation function $\sum_{m=1}^{n-1} |\rho_m|^2$ is applied for PAR reduction. This metric is additive hence is prioritized over the previous branch metric that only uses auto correlation of the side lobes.

$$\lambda(y_k) = \sum_{m=1}^{kn_s-1} |\rho_m|^2 \tag{4.2.3}$$

4.2.1 Auto-correlation representation of OFDM signal

Now, a metric that is applicable for minimizing the auto correlation of OFDM sequence's side lobes in concurrence with the viterbi algorithm as derived in [33]. Let's consider an OFDM signal $x_{(t)}$ with N-subcarriers which is expressed as:

$$x_t = \sum_{t=-\infty}^{\infty} s_l tg(t - lT_s) \tag{4.2.4}$$

Here, g_t is the windowing function and T_s refers to the symbols period. The lth complex base band OFDM symbol $s_l t$ centered at zero frequency is given by:

$$S_l t = \frac{1}{\sqrt{N}} \sum_{k=0}^{N-1} A_{t,k} e^{\frac{j2\pi(k-\frac{N-1}{2})t}{T_u}} \tag{4.2.5}$$

where $A_{l,k}$ is the complex modulated symbol after trellis shaping. From the above equation, we get [33]

$$|x_l t|^2 = \frac{1}{N} R_0 + \frac{2}{N} \sum_{m=1}^{N-1} |R_m| cos(2\pi m \frac{t}{T_u} + arg R_m) \tag{4.2.6}$$

Here, R_m shows the aperiodic auto correlation function of the complex OFDM symbol defined for $m = 0, 1, ...N-1$ as:

$$R_m \cong \sum_{k=0}^{n-1-m} A_{k+m} A_k^* \tag{4.2.7}$$

In Eq. 4.2.7, the first term is the dc component while the remaining term shows the fluctuations in the OFDM symbol envelope [33].

$$\mathbf{y} = arg \ \ min_{y \in C_s} \sum_{m=1}^{N-1} |R_m| \tag{4.2.8}$$

This helps in the selection of a code word such that the auto correlation of its side lobes are minimized. This aids in reducing the waveform fluctuations hence the dynamic range is reduced.

4.2.2 Design of metric for Viterbi algorithm

Here in, a somewhat different approach is usedd, i.e., to minimize the square of the absolute value of the side lobes which mathematically is represented as in [33]:

$$\mathbf{y} = arg \;\; min_{y \in C_s} \sum_{m=1}^{N-1} |R_m|^2 \tag{4.2.9}$$

This minimization can be made recursive. Suppose that the number of subcarriers powered by each shaping symbol be n. At the k^{th} stage, the k^{th} symbol is chosen by the equation:

$$\mathbf{y} = arg \;\; min_{y \in C_s^k} \mu_i \;, \tag{4.2.10}$$

where C_s^k is the k^{th} output symbol from C_s and μ_i is defined as:

$$\mu_i \cong \sum_{m=1}^{i-1} |R_m^(i)|^2 \tag{4.2.11}$$

where $R_m^{(i)}$ is the aperiodic auto correlation of length i complex signal. The total number of subcarriers processed up to the k^{th} stage are given by:

$$i = (k+1)\, n \;. \tag{4.2.12}$$

4.2.3 Sign-bit shaping metric

A recursive relationship can be derived for sign-bit shaping [33], which is as follows:

$$R_m^i = R_m^{(i-1)} + \sigma_m^{(i-1)} \;, \tag{4.2.13}$$

for $i = 2, 3, ...N$ and $m = 1, 2, ...i-1$.

$$\text{where} \qquad \sigma_m^{(i)} \cong A_{i-m}^* \;. \tag{4.2.14}$$

For reducing the computational complexity, the values of $\sigma_m^{(i)}$ can be computed beforehand. By substituting in the above equation, the recursive equation of μ_i becomes:

$$\mu^{(i)} = \mu^{(i-1)} + \sum_{m=1}^{i-2} 2R(R_m^{(i=1)} * \sigma_m^{(i-1)}) + \sum_{m=1}^{i-1} |\sigma_m^(i-1)|^2 \tag{4.2.15}$$

The last term in this equation shows the subcarrier symbol's power. Regardless of the chosen path, this remains constant for Type-1 mapping hence for the mapping techniques where average power reduction is not a concern, this can be omitted. The computational complexity of this metric calculation is higher than the typical viterbi decoder because it works on a recursive approach.

4.2.4 Trellis truncation to reduce complexity

The complexity of this process is mainly due to the metric calculation.For a DSP based system, complexity increases due to the complex multiplications that linearly increase. The total number of complex multiplications estimated for n_s complex-dimensional case are [33]:

$$N_{mul} = \frac{1}{2N_s} N_s(N_s - 2)(N - n_s) \tag{4.2.16}$$

This is equivalent to:

$$N_{mul} \cong \frac{N_s N^2}{2n_s} \tag{4.2.17}$$

hence the complexity is directly related to N.We therefore consider the truncated version of the auto correlation of side lobes, i.e.,

$$\mathbf{y} = arg \ \ min_{y \in C_s} \sum_{m=1}^{\delta} |R_m|^2 \tag{4.2.18}$$

where δ is the trellis window size. This complexity reduction ratio can be expressed as:

$$\eta \cong \frac{N_{mul}}{N_{mul}^{N_{mul}}} \tag{4.2.19}$$

4.2.5 Shaping codes with varying depths

Shaping codes are used to shape the $\mathcal{M}$-QAM constellation for PAPR reduction. Herein, a 256-QAM constellation with Gray mapping is considered with a shaping code of varying trellis depths. By increasing the depth of the trellis (constraint length), we may get some significant improvement in PAPR reduction. These shaping codes are characterized by their Generator matrix $\mathbf{G}$, syndrome former

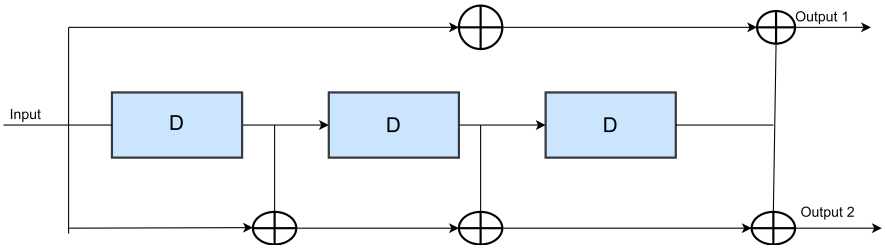

Figure 4.2: Convolutional code for (13,15)

$\mathbf{H}^T$, and its left inverse syndrome former $(\mathbf{H}^{-}1)^T$. Now let's dive straight into the multiple shaping codes that we have used here for our results.

4.2.6 The 8 states trellis (13,15) code

The (15, 17) shaping code in octal refers to (13,15) in decimal notation and forms a trellis with 8 states. The minimum hamming distance d_f for this shaping code is 6. The encoder of this system has 3 memory units or shift registers as shown in Fig. 4.2. The Generator matrix of 8-states code is defined as :

$$G = [1 + D^2 + D^3, 1 + D + D^2 + D^3] \tag{4.2.20}$$

This shaping code's parity check matrix H is:

$$[H^T] = [1 + D + D^2 + D^3, 1 + D^2 + D^3] \tag{4.2.21}$$

The syndrome former is shown in Fig. 4.3.

The syndrome former's left inverse is not unique. One of the $(H^{-1})^T$ for 8-states trellis is

$$(H^{-}1)^T = [D + D^2, 1 + D + D^2] \tag{4.2.22}$$

as shown in Fig. 4.4.

This inverse syndrome former is employed to encode the bit stream which forms the MSBs whereas LSBs are passed directly without encoding.

For the bit-error probabilities, union bound is applied for approximation. The error probabilities of the bits previously encoded by $(H^{-}1)^T$ are now found by exploiting the Union bound. The equation for union bound is based on a few parameters that are: d_{free} which is the code's minimum hamming distance, code's

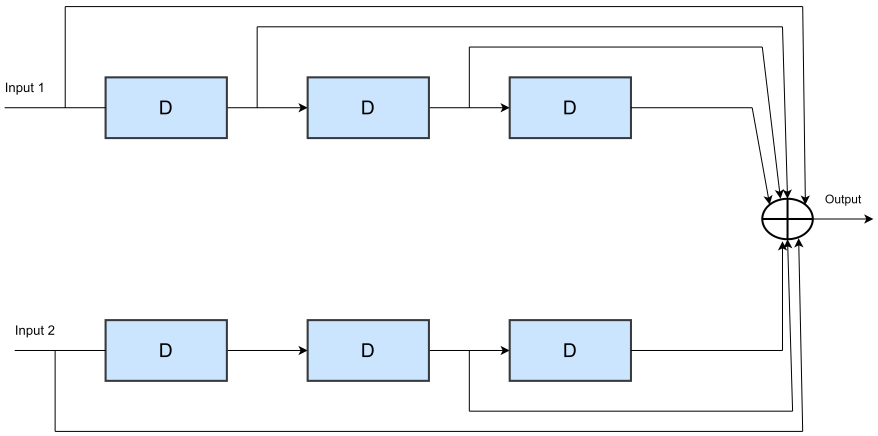

Figure 4.3: Syndrome former (13,15)

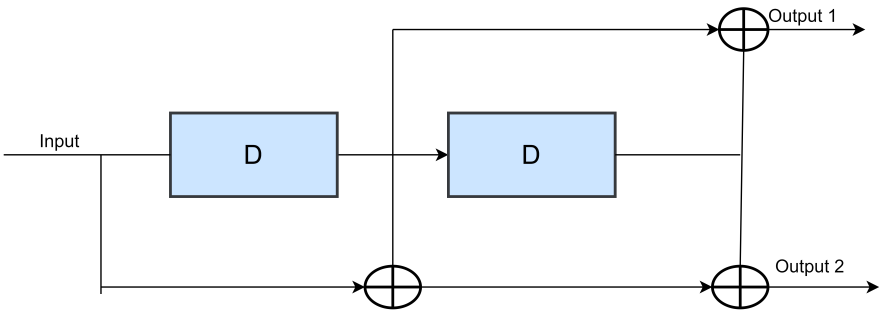

Figure 4.4: Inverse syndrome former (13,15)

weight distribution A_d, and lastly the likelihood of a wrongly chosen path at distance d p_d. The equation is as follows [42]:

$$P(b) \leq \sum_{d=d_{free}}^{\infty} A_d P_d \tag{4.2.23}$$

Summation of the error probabilities of the input bit sequence over all paths across distance d is given by union bound.

$$P(E) = \sum_{d}^{\infty} A_d P_d \tag{4.2.24}$$

The probability of choosing a wrong path at a distance d considering an AWGN channel is:

$$P_d = \frac{1}{2} erfc\left(\sqrt{\frac{E_s}{N_0} d}\right) \tag{4.2.25}$$

here, E_s/N_0 shows the signal-to-Noise ratio for an AWGN channel. The general equation for the bit-error probability is:

$$P(b) \approx \frac{1}{k}\frac{1}{2} B_{d_{free}} \left(e^{-\frac{E_s}{N_0}}\right)^{d_{free}} \tag{4.2.26}$$

For rate- 1/2 code, k=1, $B_{d_{free}}$ =1, d_{free}=3 the bit-error probability $P_{b_{s,f}}$ for the encoded bit sequence is given by:

$$P_{b_{s,f}} \approx \frac{1}{2} \left(e^{\frac{S}{N}}\right)^5 \tag{4.2.27}$$

4.2.7 The 16 states trellis (19,29) code

The (23, 35) shaping code in octal refers to (19, 29) in decimal notation and forms a trellis with 16 states. The minimum hamming distance $d_{(f)}$ for this shaping code is 7. The encoder of this system has 4 memory units or shift registers and is shown in Fig. 4.5. The Generator matrix of 16-states code is defined as

$$G = [1 + D + D^4, 1 + D^2 + D^3 + D^4] \tag{4.2.28}$$

The syndrome former, i.e., the parity check matrix **H**, as shown in Fig. 4.6 is written as

$$[H^T] = [1 + D^2 + D^3 + D^4, 1 + D + D^4] \tag{4.2.29}$$

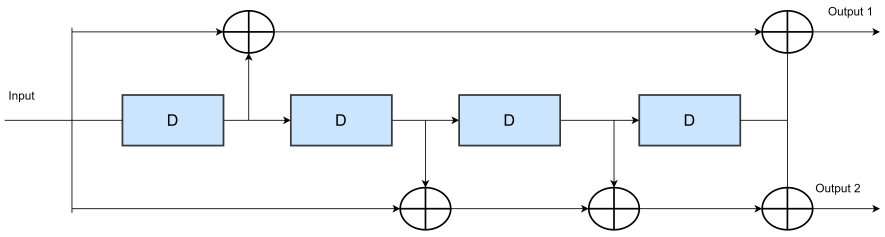

Figure 4.5: Convolutional code (19,29) code

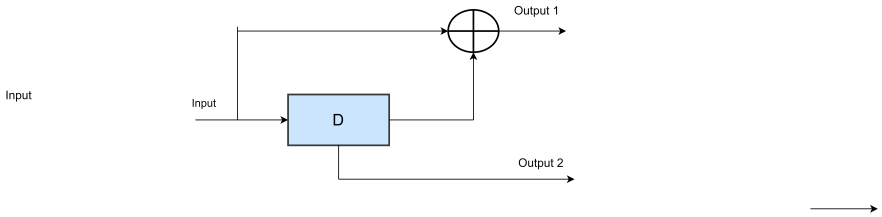

Figure 4.6: Inverse syndrome former (19,29) code

The [13,15] syndrome former's left inverse is not distinctive. One of the $(H^{-}1)^{T}$ for 16-states trellis is:

$$(H^{-}1)^{T} = [1 + D, D] \tag{4.2.30}$$

This inverse syndrome former, as shown in Fog. 4.7, is used to encode the input bit stream which forms the MSBs whereas LSBs are passed directly without encoding. The bit- error probabilities are calculated using the same equations given for 8 states trellis. The d_{free} of 16-state Trellis code is .Therefore, its bit-error probability $P_{b_{s,f}}$ is given by:

$$P_{b_{s,f}} \approx \frac{1}{2}\left(e^{\frac{S}{N}}\right)^{3} \tag{4.2.31}$$

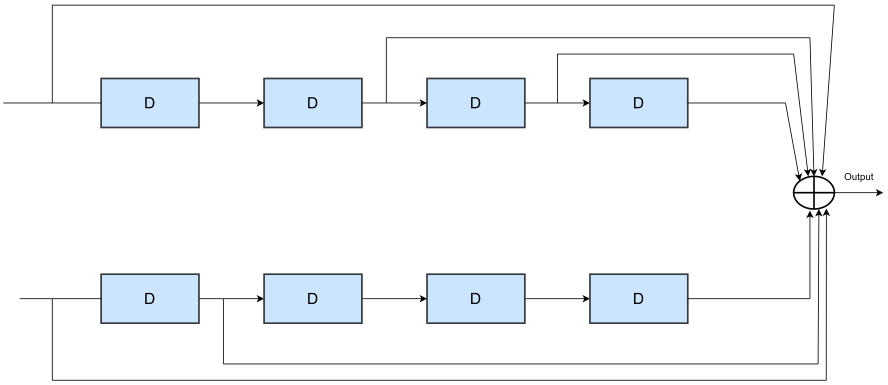

Figure 4.7: Syndrome former (19,29) code

4.2.8 The 32 states trellis (43,61) code

The (53, 75) shaping code in octal refers to (43,61) in decimal notation and forms a trellis with 32 states because the encoder for this trellis consists of 5 memory units/shift registers. The minimum hamming distance $d_{(f)}$ for this shaping code is 8 .The 32-states encoder is shown below along with its generator matrix:

$$G = [1 + D + D^3 + D^5, 1 + D^2 + D^3 + D^4 + D^5] \tag{4.2.32}$$

The syndrome former H for this shaping code is

$$[H^T] = [1 + D^2 + D^3 + D^4 + D^5, 1 + D + D^3 + D^5] \tag{4.2.33}$$

One of the $(H^{-1})^T$ for 32-states trellis is:

$$(H^-1)^T = [D^2 + D^3 + D^4, 1 + D + D^4] \tag{4.2.34}$$

This inverse syndrome former is used to encode the input bit stream which forms the MSBs whereas LSBs are passed directly without encoding. The d_{free} of 32-state Trellis code is 3 .Therefore, its bit-error probability $P_{b_{s,f}}$ is given by:

$$P_{b_{s,f}} \approx \frac{1}{2}\left(e^{\frac{S}{N}}\right)^7 \tag{4.2.35}$$

4.2.9 The 64 states trellis (91,121) code

The (133, 171) shaping code in octal refers to (91, 121) in decimal notation and forms a trellis with 64 states because the encoder for this trellis consists of 6 memory units/shift registers. The minimum hamming distance $d_{(f)}$ for this shaping code is 10 .The generator matrix $\mathbf{G}$, syndrome former $\mathbf{H}$ and the left inverse syndrome former $\mathbf{H}^{-1}$ for a 64-states shaping code can be written as

$$G = [1 + D + D^3 + D^4 + D^6, 1 + D^3 + D^4 + D^5 + D^6] \tag{4.2.36}$$

The syndrome former H for this 64-states shaping code is

$$[H^T] = [1 + D^3 + D^4 + D^5 + D^6, 1 + D + D^3 + D^4 + D^6] \tag{4.2.37}$$

One of the $(H^{-1})^T$ for this trellis shaping code is:

$$(H^-1)^T = [1 + D + D^2 + D^3 + D^5 + D^6, 1 + D + D^4 + D^6] \tag{4.2.38}$$

This inverse syndrome former is used to encode the input bit stream which forms the MSBs whereas LSBs are passed directly without encoding.

4.3 Simulation results

The simulation results of varying depths trellis shaping codes are now discussed. All the simulations are performed in MATLAB 2019. Figure:4.8 shows the plot of PAPR shaping codes with 4 and 8 states trellis depths and it is apparent that the 8-states trelis shows an improvement of 0.2dB in gain as compared to the 4-states trellis code. Figure 4.9 shows the PAPR curves trellis shaping with 4 states, 8 states, 16 states and 32 states shaping code. It is evident from the plot that increasing the trellis depth of the shaping codes, PAPR reduction is improved. This simulation is done for 256-QAM, with 128 sub-carriers and the simulation counter is set to 1000. The window size Δ is 32. A gain of almost 1.2 dB can be seen for the 32-state shaping code as compared to the4-state shaping code. Moreover, a 0.6 dB gain can be seen for the 8-state shaping, whereas, 16-state trellis shows a gain of 0.8 dB. Figure 4.9 clearly shows that higher gains can be obtained using shaping codes of higher states.

Figure 4.10 shows the BER curves for shaping codes with various depths with hard decision decoding using the syndrome former. It can be seen from the figure that there is a slight performance loss in terms of BER for shaping codes with higher number of states. Trellis shaping with 4-state shaping code has gain of 0.4 dB as compared to a trellis shaping system using 32-state shaping code.

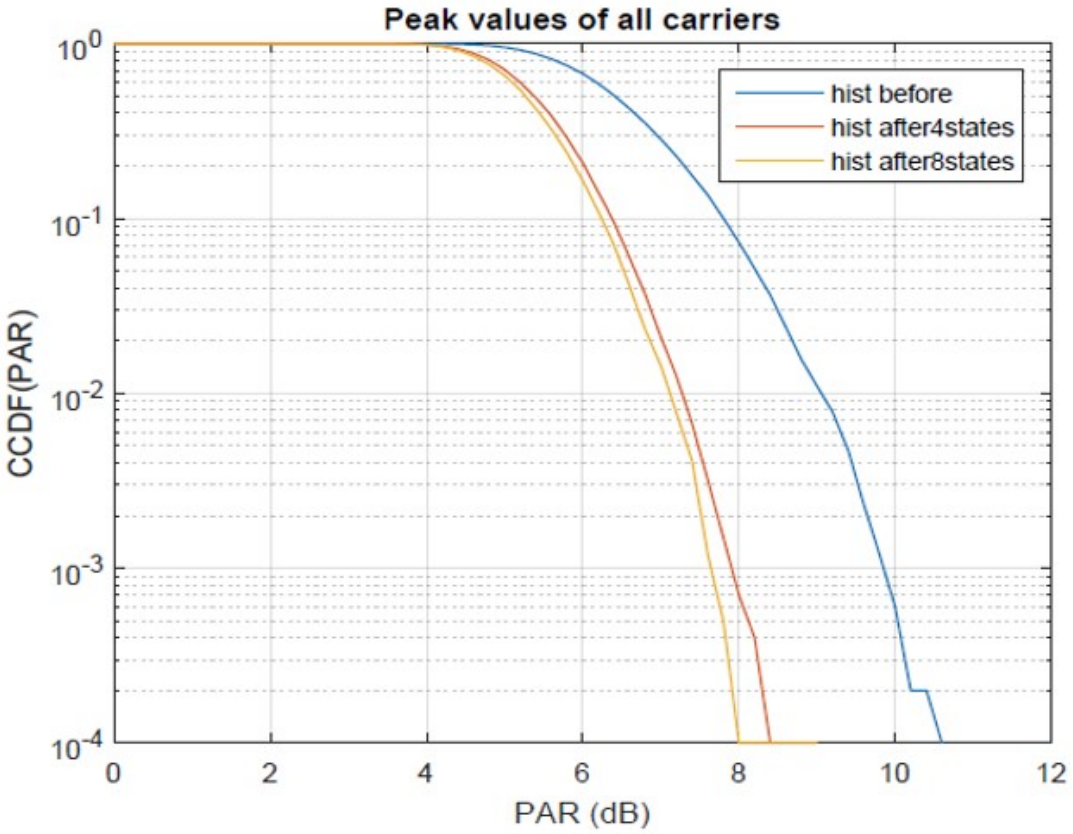

Figure 4.8: PAPR reduction with Trellis shaping for 4 and 8 states shaping code,simulation counter=10000

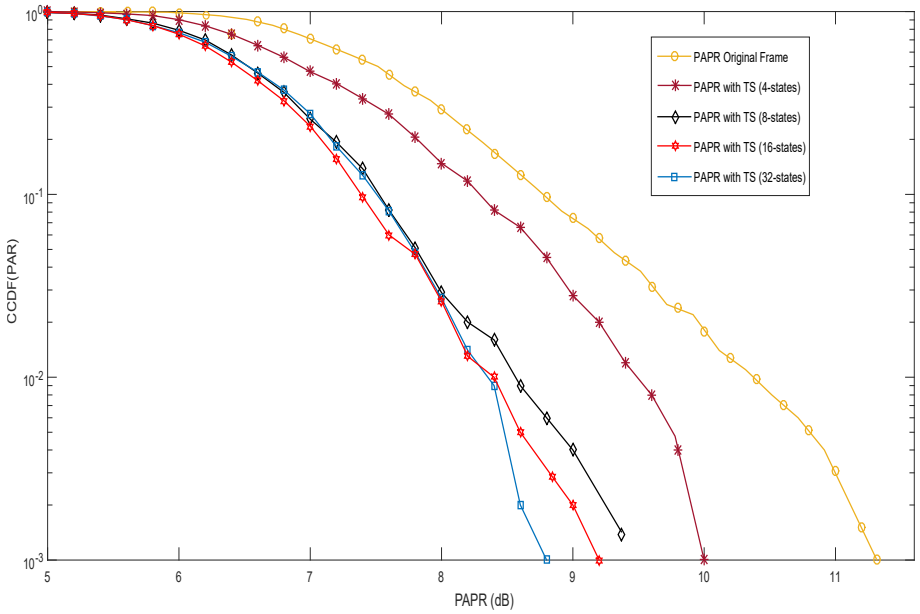

Figure 4.9: PAPR reduction using Trellis shaping with 4 , 8, 16 and 32-states shaping codes, Window size $\Delta = 32$

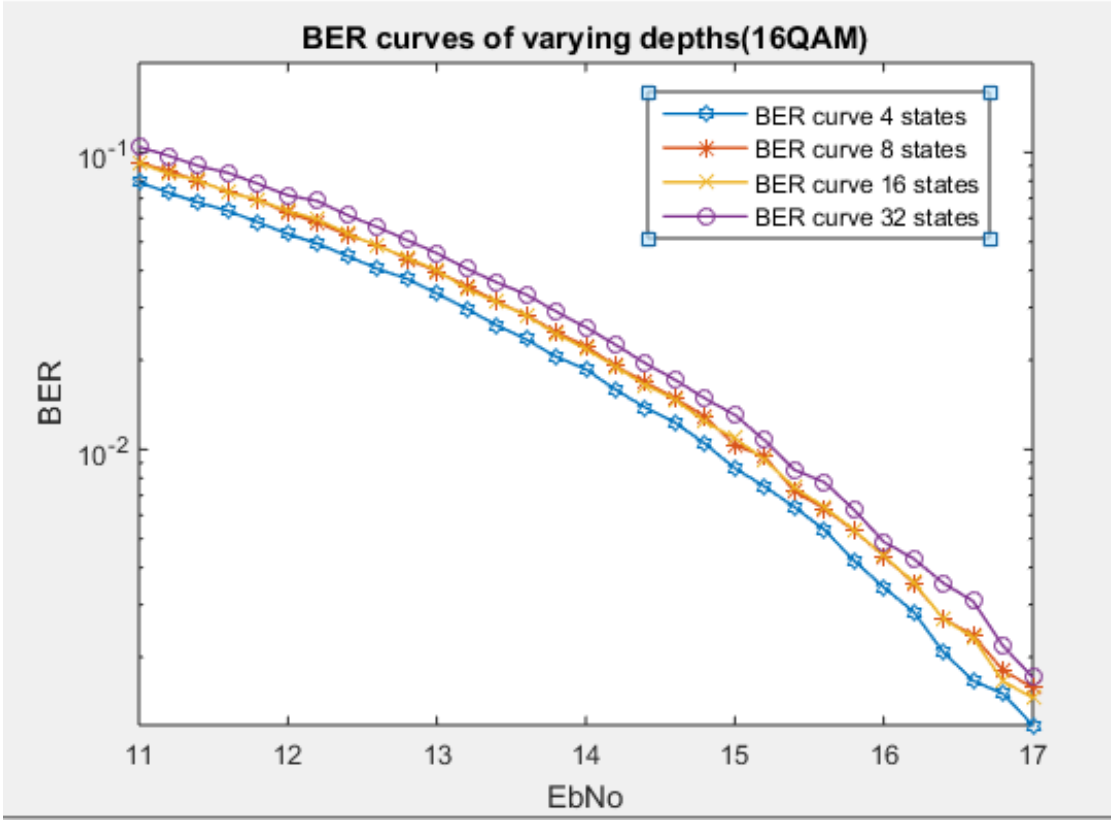

Figure 4.10: BER curves for 4 , 8 , 16 and 32-states

Chapter 5

Concatenation of optimized LDPC with Trellis shaping

In this chapter, we discuss the variable node degree distribution and its optimization algorithm. Along with this, we also discuss the LDPC code and its concatenation with trellis shaping. As the MSBs are passed through the inverse syndrome former, we also discuss briefly the multiple trellis depths used here.

5.1 Error probabilities

As far as the error probabilities of the bits are concerned,we have 8 bits per symbol here as 256 QAM constellation is used. The 8 bits can be represented as $B = b_1, b_2, b_3, ...b_8$. The individual bit error probabilities are computed as in [46].The individual probabilities can be denoted by $P_b = P_{b1}, P_{b2}, ...P_8$. As the probability of bits in the same modulation class is the same, these bit error probabilities can be grouped together as $P_b = P_{b1,2}, P_{b3,4}, P_{b5,6}, P_{b7,8}$, $P_{b1,2}$ refers to $P_{b1} = P_{b2}$, $P_{b3,4}$ refers to $P_{b3} = P_{b4}$ and so on. Here, we have 4 different error probabilities hence 4 distinct classes of modulation. The Modulation classes are $M = [M_a, M_b, M_c, M_d]$.The bit error probabilities and modulation classes can be grouped together as $P_b = [P_b, M_a, P_b, M_b, P_b, M_c, P_b, M_d]$. Later, the individual noise variances are computed for each modulation class i.e, $\sigma = [\sigma_a, \sigma_b, \sigma_c, \sigma_d]$.For

the noise variance, bit-error probabilities are used. The equation used for computing the noise variance is as follows:

$$\sigma_i^2 = \frac{1}{2erfc(2P_{b,Mi})^2} \tag{5.1.1}$$

The equation is based on the complementary error function *erfc* whereas $P_{b,Mi}$ refers to the error probability of the i-th modulation class.

5.2 Low Density Parity Check codes

The low density parity check (LDPC) codes, initially designed by Gallager, are linear block codes with very high encoding complexity but they do have several advantages over turbo codes. To begin with,the decoding of LDPC can be accomplished at relatively higher speeds.Secondly, decoders having the least complexity and that closely resemble belief propagation can be designed for these codes.Besides, the decoding of a correct code word is very much detectable.The encoding problem can somehow be limited by using a cascade of graphs instead of bipartite graphs.

Here we briefly describe some general properties of LDPC codes. They are characterized by a parity check matrix $H_{n-k\cdot n}$ where **n** shows code word length and **k** shows input vector's length.The LPDC codes are characterized by bipartite graphs having check nodes and variable nodes. The $H - matrix$ of an LDPC code consists of a few non-zero values in each column. The following conditions must be satisfied in order for a matrix to be low density.They are: $\mathbf{w_r} << \mathbf{k}$ and $\mathbf{w_c} << \mathbf{n}$. The density of the LDPC code is given by:

$$\xi_{ldpc} = w_r/n = w_c/k \tag{5.2.1}$$

LDPC code of length n is represented by an ordered pair (n, w_c, w_r). Each information bit is connected with w_c parity checks where as information bits are connected to w_r parity check bits. The number of edges connected to a node is its degree.The regular and irregular LDPC codes are differentiated by the degree of nodes.If all the variable nodes have the same degree and the check nodes have

another common degree, the code is referred to as a regular LDPC code. Regular ldpc code is specified by the ordered pair (d_v, d_c) where d_v is the variable-node degree and d_c is the check-node degree. In irregular ldpc codes, the degree of the variable and check nodes is different.For irregular code, a polynomial represents the degree distribution.These polynomials can be expressed as:

$$\lambda(x) = \sum i = 2^{d_{vmax}} \lambda_i x^{i-1} and \tag{5.2.2}$$

$$\rho(x) = \sum i = 2^{d_{cmax}} \rho_i x^{i-1} \tag{5.2.3}$$

where λ_x and ρ_x show different variable and check node distribution of degree i respectively. These polynomials are used for the code rate calculation as well.

5.3 Optimisation of Variable-node degree distribution

For optimizing the variable node degree distribution for LDPC, lets consider an Unequal Error protection (UEP) LDPC code with a code word length N. The different bit error probabilities of each bit of a QAM symbol are used for the optimization. Lets suppose that N_m represents the total number of modulation classes. The vector β_i shows the number of bits in the respective modulation class where β_i is the proportion of bits assigned to each i^{th} modulation class.The vector λ is the combined degree distribution of all the modulation classes. For the construction of an irregular LDPC codes,the check-node degree distribution is also required.The check node degree distribution is given by:

$$\rho = [\rho_2, \rho_3, ...\rho_{dc}] \tag{5.3.1}$$

5.3.1 Optimization algorithm

The variable node's degree distribution is optimized with the maximum degree i.e. $d_{v_{max}}$ despite all the constraints to have a high code rate. The process of optimization is carried out in such a way as to maximize the code rate. Here,

we briefly discuss the steps of optimization algorithm used here. Before starting the algorithm, the following values must be known: The requisite code rate R, Variance σ^2, variable node degree $d_{v_{max}}$, check node distribution ρ, along with the proportion of bits in each modulation class β. The algorithm is carried out in the following steps:

1. The proportion distribution constraint for optimization is given below:

$$\sum_{j=1}^{N_m} \sum_{i=2}^{d_{vmax}} \lambda_{M_{j,i}} = 1 \tag{5.3.2}$$

2. The convergence constraint is as follows:

$$F(\lambda, \rho, \sigma^2, x) > x \tag{5.3.3}$$

3. The stability constraint is:

$$\sum_{j=1}^{N_m} \lambda_{M_{j,2}} < \left[\sum_{j=1}^{N_m} \beta_j e^{-1/2\sigma_j^2} \cdot \sum_{m=2}^{d_{cmax}} \rho_m (m-1) \right]^{-1} \tag{5.3.4}$$

Variable node degree distribution optimized for different LDPC code ensembles concatenated with shaping codes of different depths are provided in Table 5.1.

5.4 BCJR algorithm

The inclusion of Bahl-Cocke-Jelinek-Raviv (BCJR) algorithm into the decoding process is to enhance the system performance. Previously, hard decision decoding was used at the receiver for decoding the information bit sequence. This hard decision decoding was carried out on the channel outputs in Trellis shaping as is evident from [45]. However, combining soft decision decoding to BCJR algorithm shows significant performance improvement.Therefore, we have inculcated soft decision decoding to BCJR algorithm which yields the Log-Likelihood ratios (LLRs) of the shaping bit sequence. Here Let's suppose that the QAM symbol selected by Trellis shaping is $X = [X_n], n = 1, 2, ...N,$. IFFT is performed to receive x

Table 5.1: The varying degree distributions of variable nodes for trellises with depths 4, 8, 16, and 32 states

	M_a	M_b	M_c	M_d
TS-4 states	$\lambda_3 = 0.07083$	$\lambda_3 = 0.0241$	$\lambda_2 = 0.05105$	$\lambda_2 = 0.08765$
	$\lambda_4 = 0.00013$	$\lambda_6 = 0.29473$	$\lambda_6 = 0.10195$	$\lambda_7 = 0.03643$
			$\lambda_7 = 0.09458$	$\lambda_{30} = 0.21578$
TS 8-states	$\lambda_3 = 0.07483$	$\lambda_3 = 0.0323$	$\lambda_2 = 0.07155$	$\lambda_2 = 0.08975$
		$\lambda_6 = 0.29473$	$\lambda_6 = 0.10175$	$\lambda_7 = 0.03063$
			$\lambda_7 = 0.06566$	$\lambda_{30} = 0.21588$
TS 16-states	$\lambda_2 = 0.04583$	$\lambda_7 = 0.0243$	$\lambda_8 = 0.05145$	$\lambda_4 = 0.08975$
		$\lambda_6 = 0.39473$	$\lambda_6 = 0.10605$	$\lambda_3 = 0.03603$
			$\lambda_7 = 0.09568$	$\lambda_5 = 0.21588$
TS 32-states	$\lambda_{17} = 0.08583$	$\lambda_7 = 0.0243$	$\lambda_8 = 0.05175$	$\lambda_4 = 0.08975$
		$\lambda_6 = 0.29473$	$\lambda_6 = 0.10605$	$\lambda_3 = 0.03603$
			$\lambda_7 = 0.09568$	$\lambda_5 = 0.21588$

which is then transmitted. At the DFT domain n^{th} data symbol estimated at the receiver is:

$$Y_n(Output) = X_n(Input) + w_n(Noise) \tag{5.4.1}$$

Y_n here is the n^{th} tone of the OFDM frame. At the transmitter, LSBs are mapped directly without any pre-processing therefore, the channel output directly yields LLRs for the LSBs as given below,

$$\mathcal{L}^n_{LSBs} = \ln \frac{p(c_{n,i} = 0|X)}{p(c_{n,i} = 1|X} \tag{5.4.2}$$

This shows the i^{th} received bit's probability density function (pdf) based on the n^{th} transmitted symbol.However, this approach cannot be used to obtain the LLRs of the MSBs. A combined Trellis system based on generator matrix of the shaping code C_s and $(H^{-1})^T$ i.e left inverse of syndrome former is incorporated to obtain soft outputs for the MSB information bits. The LLRs are then determined by using BCJR based on this combined trellis. The total number of states in the combined trellis is given by:

$$N_{s_{ct}} = N_{s_{cs}} \cdot N_{s_H} \tag{5.4.3}$$

The number of branches preceding from each state of combined trellis is 2^n (n is the shaping code's total number of output bits). Now,we briefly discuss the working of BCJR algorithm. For this, let $\updownarrow$ and $\updownarrow'$ be the current and previous states of a trellis respectively. Prior to the calculation of soft output of the BCJR, we first compute the forward and backward recursion and state transition probabilities. The forward recursion is given by:

$$\alpha_n(l) = \sum_{i=1}^{Ns_{ct}} \alpha_{n-1}(l'_i)\gamma_{n-1}(l'_i, l) \tag{5.4.4}$$

Similarly, the backward recursion is given by:

$$\beta_n(l') = \sum_{i=1}^{Ns_{ct}} \beta_{n+1}(l_i)\gamma_n(l', l_i) \tag{5.4.5}$$

The initial conditions are predefined for forward and backward recursions. To calculate the state transition probabilities, the equation is given below:

$$\gamma_n(l', l) = \prod_{j=1}^{2-1} p_{n,j}(l', l|X_n) \tag{5.4.6}$$

In case of no connection between l' and l then $\gamma_n(l', l)$ is equal to 0. After getting all the above data i.e. forward and backward recursions and state transitions, the likelihood for j^{th} received bit of the MSBs is computed by:

$$p(z_n'^j = b, X) = \sum_{\zeta \in \Upsilon(b)} \alpha_n(l')\gamma_n(l', l)\beta_{n+1}(l) \tag{5.4.7}$$

where $z_n'^j$ is the received j^th symbol belonging to the MSBs.Finally, the LLRs are calculated by:

$$\mathcal{L}^n_{MSBs} = \ln \frac{p(z_n'^j = 0|X)}{p(z_n'^j = 1|X} = \ln \frac{p(z_n'^j = 0, X)}{p(z_n'^j = 1, X} \tag{5.4.8}$$

The LLRs of both MSBs and LSBs are fed into LDPC decoder to retrieve information for the entire bit sequence u.

5.5 Results and Discussion

Single-input Single-output (SISO) OFDM system is considered here which is appended to a rate - k/n LDPC code. For simulation results, a 256-QAM constellation with Gray mapping. The LDPC codes used are both regular and irregular with a rate 6/7 to achieve a higher spectral efficiency. Here we have considered 256 QAM modulation for an OFDM frame of 128 subcarriers. As we already know that each 256 QAM symbol comprises of 8 bits per symbol, the bits required to match one OFDM frame are 8 x 128= 1024 bits. One redundant bit per symbol is added by the Trellis shaping block appended with LDPC code. Therefore, matching the size of LDPC with one OFDM frame, requires LDPC code to be picked-out as 896 (896 + 128 =1024). This makes the system's collective code rate equal to 3/4. Belief Propagation (BP) is used with maximum iterations 30 for LDPC code word decoding. For regular and irregular LDPC, the maximum iterations limit is 30. For comparison of our results with system without Trellis shaping, the code word length is set to 1024 and code rate is 3/4. The LDPC and Trellis shaping combined system is shown in Fig: 5.1.

Now lets see how this system works. Encoding of the input bit stream 'u' is done with with irregular LDPC code. The individual bits inside the M-ary QAM

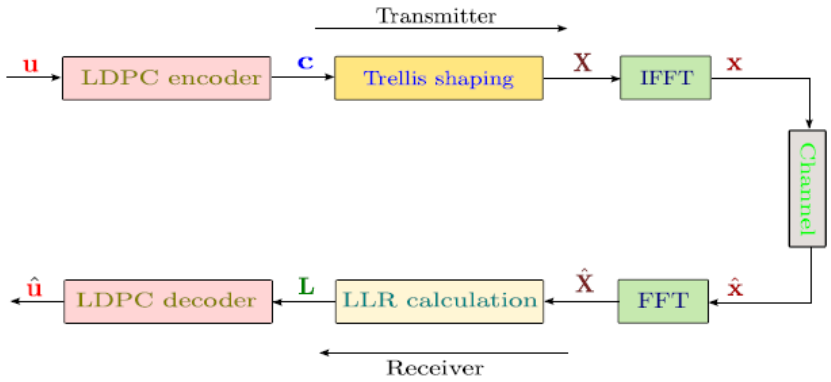

Figure 5.1: Irregular LDPC and TS concatenated system

symbol are used for LDPC code optimization i.e the bit error probabilities of each bit are exploited for optimization. As its obvious from our previous discussion that irregular LDPC codes outperform the regular LDPC codes. In Fig: 5.2 we compare regular and Irregular LDPC codes. Herein, we consider a (3, 21) regular LDPC code. This has the same code rate as that of irregular LDPC codes. Fig:5.2 shows the performance analysis of regular Vs Irregular LDPC codes using 4 states and 8-states shaping codes. For the variable node degree optimization, we exploited the error probabilities calculated for different shaping codes using union bound in Chapter-4. The variable node degree distribution obtained for various shaping codes are given in Table-1. Figure 5.2 show the BER curves for regular and irregular LDPC codes using 4-states and 8-states shaping codes. It can be seen that the system performance improves using shaping codes of larger depths. The system performance is improved by 0.2 dB using 8-states shaping as compared to the one using 4-states shaping code as shown in Fig. 5.2.

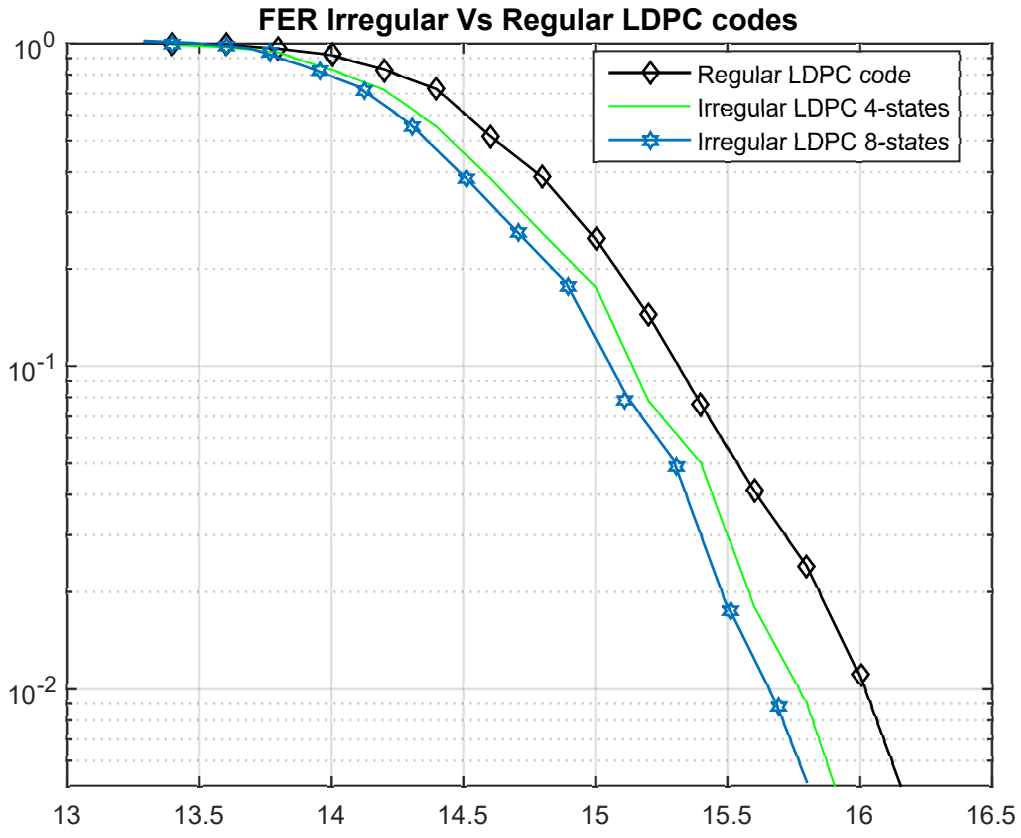

Figure 5.2: Regular Vs Irregular LDPC 896

Chapter 6

Conclusion

Herein, we used trellis shaping for PAPR reduction in SISO systems. For PAPR reduction using trellis shaping, we have used shaping codes of various depths. The simulation results shows that the system performance in terms of PAPR can be improved using shaping codes of larger depths. However, the gain is obtained at the expense of a sight increase in the system computational complexity. Moreover, BER curves are evaluated for different shaping codes, which shows that the BER penalty for obtaining the gain is marginal, i.e., 0.4 dB for shaping code with 16 states trellis depth. To improve the system performance in terms of BER, we concatenate an irregular LDPC code with trellis shaping using different depths. For irregular LDPC codes, the variable node degree distribution was optimized by exploiting the error probabilities of various shaping codes obtained using union bounds. It can be seen that the the results for larger depth shaping codes concatenated with trellis shaping performs better than the 4-states shaping code.

References

[1] Kim, Haesik. Design and Optimization for 5G Wireless Communications. John Wiley & Sons, 2020.

[2] Hanna Bogucka, Adrian Kliks, Pawel Kryszkiewicz, References, Advanced Multicarrier Technologies for Future Radio Communication, 10.1002/9781119168935, (251-282), (2017).

[3] Shidong Zhou, Ming Zhao, Xibin Xu, Jing Wang and Yan Yao, "Distributed wireless communication system: a new architecture for future public wireless access," in IEEE Communications Magazine, vol. 41, no. 3, pp. 108-113, March 2003, doi: 10.1109/MCOM.2003.1186553.

[4] Shanmugam, K. Sam. "Digital and analog communication systems." NASA STI/Recon Technical Report A 80 (1979): 23225.

[5] G. Gu and G. Peng, "The survey of GSM wireless communication system," 2010 International Conference on Computer and Information Application, Tianjin, China, 2010, pp. 121-124, doi: 10.1109/ICCIA.2010.6141552.

[6] Hwang, Taewon, Chenyang Yang, Gang Wu, Shaoqian Li, and Geoffrey Ye Li. "OFDM and its wireless applications: A survey." IEEE transactions on Vehicular Technology 58, no. 4 (2008): 1673-1694.

[7] Y. Liu, Z. Tan, H. Hu, L. J. Cimini and G. Y. Li, "Channel Estimation for OFDM," in IEEE Communications Surveys & Tutorials, vol. 16, no. 4, pp. 1891-1908, Fourthquarter 2014, doi: 10.1109/COMST.2014.2320074.

[8] T. Lee and H. Ochiai, “Characterization of power spectral density for nonlinear amplified OFDM signals based on cross-correlation coefficient,” EURASIP Journal of Wireless Communications and Networking, 2014.

[9] Saxena, Rajiv, and Hem Dutt Joshi. "OFDM and its major concerns: a study with way out." IETE Journal of Education 54, no. 1 (2013): 26-49.

[10] Baig, Imran, and Varun Jeoti. "PAPR reduction in OFDM systems: Zadoff-Chu matrix transform based pre/post-coding techniques." In 2010 2nd International Conference on Computational Intelligence, Communication Systems and Networks, pp. 373-377. IEEE, 2010.

[11] J. Andrews, S. Buzzi, W. Choi, S. Hanly, A. Lozano, A. Soong, et al., "What will 5G be?", Selected Areas in Communications IEEE Journal on, vol. 32, no. 6, pp. 1065-1082, June 2014.

[12] W. Xiang, K. Zheng and X. Shen, Key Enabling Technologies for 5G Mobile Communications., Springer, 2016.

[13] F.-L. Luo and C. Zhang, Signal Processing for 5G: Algorithms and Implementations., Wiley, 2016.

[14] Litsyn, Simon. Peak power control in multicarrier communications. Cambridge University Press, 2007.

[15] Al-Jawhar, Yasir Amer, Khairun N. Ramli, Montadar Abas Taher, Nor Shahida M. Shah, Salama A. Mostafa, and Bashar Ahmed Khalaf. "Improving PAPR performance of filtered OFDM for 5G communications using PTS." ETRI Journal (2020).

[16] Cui, Tao, and Chintha Tellambura. "Semiblind channel estimation and data detection for OFDM systems with optimal pilot design." IEEE Transactions on Communications 55, no. 5 (2007): 1053-1062.

[17] Taha, Haitham J., and M. F. M. Salleh. "Multi-carrier transmission techniques for wireless communication systems: A survey." Wseas transactions on communications 8, no. 5 (2009): 457-472.

[18] R. V. Nee, G. Awater, M. Morikura, H. Takanashi, M. Webster and K. W. Halford, "New high-rate wireless LAN standards", IEEE Commun. Mag., vol. 37, no. 12, pp. 82-88, December 1999.

[19] M. A. Saeed, B. M. Ali and M. H. Habaebi, "Performance evaluation of OFDM schemes over multipath fading channels," 9th Asia-Pacific Conference on Communications (IEEE Cat. No.03EX732), Penang, Malaysia, 2003, pp. 415-419 Vol.1, doi: 10.1109/APCC.2003.1274387.

[20] R. W. Chang, “Synthesis of band-limited orthogonal signals for multichannel data transmission,” Bell Syst. Tech. J., vol. 45, pp. 1775–1797,Dec. 1966.

[21] B. Hirosaki, S. Hasegawa, and A. Sabato, “Advanced groupband data modem using orthogonally multiplexed QAM technique,” IEEE Trans.Commun., vol. COM-34, no. 6, pp. 587–592, Jun. 1986.

[22] A. Peled and A. Ruiz, “Frequency domain data transmission using reduced computational complexity algorithms,” in Proc. IEEE Int. Conf. Acoust., Speech Signal Process., 1980, pp. 964–967.

[23] C.D. Chung, Spectrally Precoded OFDM, IEEE Transactions on Communications, VOL. 54, NO. 12, DECEMBER 2006, pp. 2173-2185.

[24] S. U. Hwang, J. H. Lee, and J. Seo, Low Complexity Iterative ICI Cancellation and Equalization for OFDM Systems Over Doubly Selective Channels, IEEE Transactions on Broadcasting, VOL. 55, NO. 1, MARCH 2009 , pp. 132-139.

[25] Taha, Haitham J., and M. F. M. Salleh. "Multi-carrier transmission techniques for wireless communication systems: A survey." Wseas transactions on communications 8, no. 5 (2009): 457-472.

[26] S. B. Weinstein, "The history of orthogonal frequency-division multiplexing [History of Communications]," in IEEE Communications Magazine, vol. 47, no. 11, pp. 26-35, November 2009, doi: 10.1109/MCOM.2009.5307460.

[27] Mubeen, S., Prasad, A.M., and Rani, A.J. (2012). Smart Antenna Implementation for MIMO. Journal of Information Engineering and Applications, 2(4), 9-16.

[28] Venkateswarlu, P., and Nagendra, R. (2014). Channel Estimation Techniques in MIMO-OFDM LTE Systems. Int. Journal of Engineering Research and Applications, 4(7), 157-161.

[29] Kumar, K.S., Munawwar, S., and Mohan Reddy, M. (2019). Performance of MIMO in the Presence of Different Noises and Different Modulation Techniques. International Journal of Management, Technology and Engineering, 9(1), 2227-2235.

[30] Khanzadi, M.R., Durisi, G., and Erikson, T. (2015). Capacity of SIMO and MISO Phase-Noise Channels with Common/Separate Oscillators. IEE Transactions on Communication, arXiv:1409.0561v3 [cs.IT] 24 Feb 2015, 1-13.

[31] Shreelakshmi, C. S., Shettar, N. S., and Srikantan, A.V. (2016). Adaptive monitoring technique for MIMO-OFDM systems. GSSS Institute Of Engineering And Technology For Women, Mysuru , National Level PG Project Symposium On Electronics and Communication, Computer Science, 1-4.

[32] Mohinder Jankiraman, "Peak to average power ratio," in Space-time codes and MIMO systems, Artech House, pp. 201, 2004

[33] H. Ochiai and H. Imai, "On the clipping for peak power reduction of OFDM signals," in Proc. IEEE Global Communications Conference (GLOBECOM), San Francisco, USA, 2000, pp. 731–735.

[34] S. K. Deng and M. C. Lin, "Recursive clipping and filtering with bounded distortion for PAPR reduction," IEEE Trans. Commun., vol. 55, no. 1, pp. 227–230, January 2007.

[35] Y. C. Wang and Z. Q. Luo, "Optimized iterative clipping and filtering for PAPR reduction of OFDM signals,"

[36] D. Kim, D. Shi, Y. Park, and B. Song, “New peak-windowing for PAPR reduction of OFDM systems,” in Proc. Asia-Pacific Conference on Wearable Computing Systems (APWCS), August 2005, pp. 169–173.

[37] H. Xiao, L. Jianhua, C. Justin, and Z. Junli, “Companding transform for the reduction of peak-to-average power ratio of OFDM signals,” in Proc. IEEE Vehicular Technology Conference (VTC), 2001, pp. 835– 839.

[38] “DMT PAR-reduction by weighted cancellation waveforms,” in Proc. Radiovetenskap och kommunikation 99 (RVK 99), Karlskrona, Sweden, June 1999, pp. 303–307.

[39] S. Y. Le Goff, B. K. Khoo, C. C. Tsimenidis and B. S. Sharif, "A novel selected mapping technique for PAPR reduction in OFDM systems," in IEEE Transactions on Communications, vol. 56, no. 11, pp. 1775-1779, November 2008, doi: 10.1109/TCOMM.2008.070021.

[40] G. D. Forney Jr., “Trellis shaping,” IEEE Trans. Inform. Theory, vol. 38, pp. 281–300, Mar. 1992.

[41] W. Henkel and B. Wagner, “Another application for trellis shaping:PAR reduction for DMT(OFDM),” IEEE Trans. Commun., vol. 48, no. 11, pp. 1471–1476, September 2000.

[42] H. Ochiai and H. Imai, “Performance analysis of deliberately clipped OFDM signals,” IEEE Trans. Commun., vol. 50, pp. 89–101, Jan. 2002.

[43] T. T. Nguyen and L. Lampe, “On trellis shaping for PAR reduction in OFDM systems,” IEEE Trans. Commun., vol. 55, no. 9, pp. 1678–1682, September 2007.

[44] S. Fei, Y. Yong, Z. Shijie, and S. Dechun, “A novel PAPR reduction with Trellis Shaping in NC-OFDM in cognitive radio,” Journal of Electronics (China), Vol. 26, No. 3, pp. 296-302, May 2009

[45] H. Ochiai, “A novel Trellis-Shaping design with both peak and average power reduction for OFDM systems,” IEEE Transactions on Communications, Vol. 52, No. 11 pp. 1916-1926, November 2004.

[46] D. Yoon, K. Cho, and J. Lee, “Bit error probability of M-ary quadrature amplitude modulation,” Vehicular Technology Conference, Massachusetts, USA, September 2000.

[47] Wakeel, Abdul. "Peak-to-Average Ratio Reduction for MIMO and Multi-user OFDM Systems." PhD diss., Jacobs University Bremen, 2016.